Published in final edited form as:
*Cerebellum*. 2011 June ; 10(2): 254–266. doi:10.1007/s12311-011-0262-5.

# Glial S100B protein modulates mutant ataxin-1 aggregation and toxicity: TRTK12 peptide, a potential candidate for SCA1 therapy

**Parminder J.S. Vig**[1,2,*], **Scoty Hearst**[1,2], **Qingmei Shao**[1], **Maripar E Lopez**[1], **Henry A Murphy II**[1], and **Eshan Safaya**[1]

[1]Department of Neurology, University of Mississippi Medical Center, Jackson, Mississippi 39216

[2]Department of Biochemistry, University of Mississippi Medical Center, Jackson, Mississippi 39216

## Abstract

Non-cell autonomous involvement of glial cells in the pathogenesis of polyglutamine diseases is gaining recognition in the ataxia field. We previously demonstrated that Purkinje cells (PCs) in polyglutamine disease spinocerebellar ataxia-1 (SCA1) contain cytoplasmic vacuoles rich in Bergmann glial (BG) protein S100B. The vacuolar formation in SCA1 PCs is accompanied with an abnormal morphology of dendritic spines. In addition, S100B mRNA expression levels are significantly high in the cerebella of asymptomatic SCA1 transgenic (Tg) mice and increase further with age when compared with the age-matched wildtype animals. This higher S100B mRNA expression positively correlates with an increase in the number of vacuoles. To further characterize the function of S100B in SCA1 pathology, we explored the effects of S100B protein on GFP-ataxin-1 (ATXN1) with expanded polyglutamines [82Q] in HEK stable cell line. Externally added S100B protein to these cells induced S100B positive vacuoles similar to those seen in SCA1 PCs *in vivo*. Further, we found that both externally added and internally expressed S100B significantly reduced GFP-ATXN1[82Q] inclusion body formation. In contrast, the addition of S100B inhibitory peptide TRTK12 reversed S100B mediated effects. Interestingly, in SCA1 Tg mice, PCs containing S100B vacuoles also showed the lack of nuclear inclusions, whereas, PCs without vacuoles contained nuclear inclusions. Additionally, TRTK12 treatment reduced abnormal dendritic growth and morphology of PCs in cerebellar slice cultures prepared from SCA1 Tg mice. Moreover, intranasal administration of TRTK12 to SCA1 Tg mice reduced cerebellar S100B levels in the particulate fractions and these mice displayed a significant improvement in their performance deficit on the Rotarod test. Taken together our results suggest that glial S100B may augment degenerative changes in SCA1 PCs by modulating mutant ataxin-1 toxicity/solubility through an unknown signaling pathway.

### Keywords

Purkinje cells; S100B; ataxin-1; spinocerebellar ataxia-1; cerebellum; vacuoles; neurodegeneration; Bergmann glia

[*]Correspondence should be addressed to: Dr. P.J.S. Vig, Department of Neurology, University of Mississippi Medical Center, 2500 North State Street, Jackson, MS 39216, Ph: 601-984-5513, Fax: 601-984-6626, pvig@neurology.umsmed.edu.

**Conflict of Interest (COI) Statement:**
There is no conflict of interest. The data reported in this manuscript has not been published or submitted for publication elsewhere. All authors have agreed to the contents of this article and there are no ethical issues involved.

## Introduction

Spinocerebellar ataxia type1 (SCA1) is an autosomal dominant neurodegenerative disorder characterized by progressive ataxia due to the loss of cerebellar Purkinje cells (PCs) and neurons in the brainstem [1–3]. A polyglutamine expansion in the disease causing protein ataxin-1 is known to be the major player in neuronal degeneration; however, the exact function of mutant ataxin-1 is still debated [2,4,5]. In B05 SCA1 transgenic (Tg) mice, the expression of mutant ataxin-1 transgene PS-82 produces progressive ataxia and PC pathologic changes mirroring those seen in SCA1 patients [6]. In these mice, the most prevalent features of SCA1 disease are the development of cytoplasmic vacuoles and the presence of nuclear inclusions in PCs. However, vacuole development precedes both nuclear inclusion formation and behavioral abnormalities [7–9]. Recently, we reported that Bergmann glia (BG) protein S100B localizes to SCA1 PC vacuoles in both SCA1 Tg mice and SCA1 patients and vacuolar formation is associated with abnormal PC morphology [8,9]. The mechanistic link between mutant ataxin-1 expression and S100B vacuole development is not well established yet and needs further investigation.

The astrocytic S100B protein belongs to the EF-hand family of calcium binding proteins [10,11]. S100B is abundantly expressed in the nervous system and can function as a neurotrophic signaling molecule or as a neurotoxic agent [11–14]. Neurotrophic expression of S100B promotes neuronal survival and development [15–17]. Increased levels of S100B have also been reported in brain injury, Alzheimer's disease and Down syndrome [14,18,19]. S100B has been shown to interact with multiple protein targets including p53, nuclear Dbf2-related kinases, receptor for advanced glycation end products, protein kinase C, neuromodulin, and myo-inositol-monophosphatase-1 [9,20–22].

Cell bodies of BG are located in the PC layer of the cerebellar cortex. BG form rosettes around PCs, ensheathe their dendrites and synapses to maintain and regulate PC structure and function respectively [23,24]. BG climbing fibers are said to guide granule cell migration during cerebellum development and to provide a scaffold for growing PC dendritic arborizations [23]. Damaged BG have been shown to cause degeneration of PC dendrites, granule cell death and impaired motor coordination [25]. We also indicated earlier [9] that BG may mediate SCA1 pathology via S100B vacuoles, which localize to PC cytoplasm and demonstrated that PCs with vacuoles show severe atrophy of dendrites and spines as compared to cells without vacuoles [9]. Our data is supported by a recent report on SCA1 knockin mice suggesting that functional deficiency of BG may contribute to PC pathology in SCA1 [26]. Similar alterations in PCs were seen when ataxin-7 was expressed in BG in SCA-7 mouse model [27]. We believe that BG dependent pathways initiating PC death may be common to multiple neurodegenerative diseases. In this study, we further characterize the role of BG in SCA1 pathogenesis and show that S100B protein may directly influence ataxin-1 toxicity and/or solubility.

## Materials and Methods

### Materials

Paraformaldehyde (PFA), biochemicals and culture media were purchased from Sigma-Aldrich (St. Louis, MO, USA). Fetal bovine serum (FBS) was purchased from HyClone (Logan, UT, USA). Fugene 6 transfection reagent and green fluorescent protein (GFP) antibody were purchased from Roche (Indianapolis, IN, USA). S100B antibody was purchased from Abcam (Cambridge, MA, USA). S100B protein was purchased from Sigma-Aldrich. Ubiquitin antibody was purchased from Santa Cruz Biotechnology (Santa Cruz, CA, USA). TRTK12 and 5FAM labeled TRTK12 peptides were purchased from AnaSpec (San Jose, CA, USA).

### Cell culture and transfections

HEK and HeLa cells (Invitrogen, Carlsbad, CA, USA) were maintained in Dulbecco's modified Eagle's medium (Fisher, Houston, TX, USA) supplemented with 10% FBS, penicillin-streptomycin, and grown in an incubator at 37°C in the presence of 5% CO2. GFP-ataxin-1[82Q], mammalian expression vector was kindly provided by Dr. Huda Zoghbi, Howard Hughes Medical Institute, Baylor College of Medicine TX, USA [28–30]. S100B expression vector was generously provided by Dr. Kim Neve, Department of Behavioral Neuroscience, Oregon Health & Science University and Portland Veterans Affairs Medical Center, Portland, OR, USA [31]. HEK cells were transfected using Fugene 6 transfection reagent (Roche) according to manufacturer's guide lines to express GFP-ataxin-1[82Q] followed by selection with G418 antibiotic (G418 sulfate 600 μg/ml, Sigma) to produce GFP-ataxin-1[82Q] stable cell lines. HeLa cells were transfected using Fugene 6 transfection reagent to express S100B followed by selection with G418 antibiotic to produce S100B stable cell lines.

### Immunofluorescence, co-immunoprecipitation, and Western blotting

GFP-ataxin-1[82Q] HEK cells were transferred to 2 well chamber slides (Fisher) and treated with 500nM S100B for 24hrs. HeLa cells placed on 2 well slides were treated with Alexa-594-S100B. Bovine S100B protein (Sigma) was labeled with Alexa-594 dye using Alexa-Fluor-594 protein labeling kit (Invitrogen) according to the manufacturer's guide lines. Slides were fixed with 4% PFA and probed with appropriate GFP or S100B antibodies and fluorescent secondary antibodies Alexa 488 and Alexa 546 (Invitrogen). Cells were observed on an Olympus BX60 epi-fluorescence microscope. GFP-ataxin-1[82Q] inclusions in the transfected cells were scored according to the method described by Parfitt and co-workers [32] as soluble (diffuse localization within the nucleus), as small punctuate foci, or as larger inclusions [32]. For each group of cell culture experiment, around 100 cells were counted per treatment group and each experiment was repeated for a total of three times. Averages and standard errors were taken and statistics were calculated using the Student's t-test. For Western blotting, cells were lysed in RIPA buffer (50 mM Tris-HCl, pH 7.5, 150 mM NaCl, 1 mM EDTA, 1% sodium deoxycholate and 1% NP-40, Sigma), followed by brief sonication as previously described [33]. Co-immunoprecipitation of S100B and GFP-ataxin-1 was performed using Seize X Protein A Plus IP kit (Pierce, Rockford, IL, USA) as previously described [9]. Bead bound proteins were mixed with SDS-PAGE sample buffer, followed by boiling for 5 minutes. Samples were resolved by SDS-PAGE as previously described [9].

### SCA1 Transgenic Mice

The SCA1 Tg mice were generated and kindly provided by Drs. Harry Orr and Huda Zoghbi [6]. Colonies of SCA1 Tg mice are maintained in our animal facility. The heterozygous PS-82 BO5 line of mice were identified using a transgene specific polymerase chain reaction assay and were backcrossed to the parental FVB/N strain (N=10) to establish congenic line with homogeneous background strain [9]. The line B05 expresses 30 copies of the transgene PS-82. B05 Tg mice develop progressive loss of PCs and cerebellar function. Heterozygous B05 mice become visibly ataxic at 12 weeks of age and homozygous B05 mice show ataxia at 6 weeks of age.

### Green fluorescent protein (GFP) transgenic mice

Homozygous GFP mice and wildtype (same background) were obtained from Jackson Labs, Bar Harbor, Maine. We have a colony of GFP transgenic mice in our animal facility [9]. The transgene expression of Enhanced GFP gene is under the control of pcp2/L7 promoter similar to ataxin-1 expression in SCA1 mice, GFP is expressed only in Purkinje cells, where

it fills dendrites, soma, axons and nuclei. GFP is detected in PCs as early as E17 and increases during development. There is no PC pathology or behavioral abnormalities in these mice.

## Generation of experimental animals

**SCA1: GFP mice—**Female mice (FVB/N) homozygous for SCA1 (SCA1/SCA1) were mated with male (FVB/N) homozygous (GFP/GFP) GFP mice to generate double mutants heterozygous for both SCA1 and GFP (SCA1/+: GFP/+).

**Wildtype: GFP—**Homozygous GFP (GFP/GFP) males (FVB/N) were mated with wildtype (+/+) females FVB/N) to generate heterozygous (GFP/+) mice wildtype for SCA1.

The manipulation and maintenance of animals were approved by the Institutes Animal Care and Use Committee This committee enforces the regulations for using animals in scientific research at the University of Mississippi Medical Center (UMMC), Jackson, MS, USA.

## Purkinje Cell Cultures

Cerebellar slice cultures were prepared from 7–11 day old SCA1 Tg mouse pups. The whole cerebella were obtained after sacrifice and meninges were carefully removed using a dissection microscope. Tissue was rinsed and placed in Petri dishes containing 5% glucose and cold Gey's balanced salt solution (Gey solution, Sigma). Cerebellar tissues were cut into 250 μm slice sections using a McIlwain tissue chopper. Cerebellar slices were resuspended in cold Gey solution containing 5% glucose, then grown on Millicell membrane inserts (Fisher) using 6-well culture plate containing 1 ml plating media (for 100 ml media: 5 ml 10X Basal Medium with Earle's Salt, 2.5 ml 10X HBSS, 25 ml Horse Serum (Invitrogen), 1 ml 100X Pen-Strep-Glutamine, 4.5 ml 10% D-Glucose, 0.5 ml 7.5% Sodium bicarbonate and 61.5 ml sterile water, Sigma). Tissue cultured plates were incubated overnight at 35.5°C with 5% CO2 and 100% humidity. The next day, cells were flushed and treated with various concentrations of TRTK12 in plating media. Cultures were fixed in 4% PFA, placed on plus slides (Fisher) and then immunostained using GFP antibody followed by fluorescent secondary antibody Alexa 488. Tissues were observed on an Olympus BX60 epi-fluorescence microscope.

## End Point and Real Time PCR

RNA from whole cerebellar homogenates was isolated from 2 and 4 week old FVB WT and SCA1 Tg heterozygous (Het) mice using the Absolutely RNA mini prep kit (Stratagene). The RNA quality was measured by Lab Chip RNA 6000 Nano Assay (Agilent Technologies, Santa Clara, CA, USA) using the UMMC core facility MFGN INBRE Program of the National Center for Research Resources (NIH Grant Number RR 016476-09A1). Next, 2μg of RNA was used to produce cDNA using the High Capacity RNA-to-cDNA Kit (Applied Biosystems, Foster City, CA, USA). S100B and β-Actin primers (IDT, San Jose, CA, USA) were used to amplify the cDNA for 30 cycles using the Taq PCR kit (Qiagen, Valencia, CA, USA) and a PCR machine. S100B forward primer: CTGGAGAAGGCCATGGTTGC, S100B reverse primer: CTCCAGGAAGTGAGAGAGCT, product size, 110bp, β-Actin forward primer: GTGGGCCGCTCTAGGCACCAA, β-Actin reverse primer: CTCTTTGATGTCACGCACGATTTC, product size, 540bp. Amplified DNA was run on a 2% agarose gel containing 0.005% ethidium bromide. The DNA gel was visualized using a UV Bio-Rad Imaging Station (Bio-Rad Laboratories, Hercules, CA, USA). Band intensity values were taken using ImageJ software. Graph displays the MEAN±SE of the relative mRNA levels of S100B compared to β-Actin. Statistical analysis was calculated using the Student's t-test. cDNA was then used for real-time PCR using Fast EvaGreen qPCR Master

Mix (Biotium, Hayward, CA, USA) and the reactions were subjected to a 10 minute incubation at 95°C, followed by 40 amplification cycles (95°C for 30 seconds, 50°C for 30 seconds, 72°C for 1 minute) and a dissociation curve-analysis step. The reactions were conducted using a MX3000P or a MX3005P real-time PCR system (Strategene, Cedar Creek, TX, USA). Amplification rates, Ct values and dissociation curve analyses of products were determined using MxPro (version 4.01) software. Relative expression was determined using the $2(-\Delta\Delta Ct)$ method [34]. Student's t-test was used to determine statistical significance and P value of less than 0.05 was considered as statistically significant.

### Tissue Processing

Spinocerebellar ataxia 1 Tg heterozygous, homozygous or double Tg (SCA1: GFP) mice at different postnatal days were anesthetized and perfused with 4% buffered PFA according to the method described by Neuroscience Associates, Knoxville, TN, USA. The brains were removed and immersed in the perfusion fixative then transferred to phosphate-buffered saline and processed for vibratome sectioning or paraffin embedding as previously described [9]. Sections were cut from the midline sagittal plane of the cerebella. Sections were double immunostained for ubiquitin and S100B using the immunohistochemical protocol as previously described [9].

### Intranasal administration of TRTK12

2 week old GFP: SCA1 animals were randomly divided into two treatment groups. The TRTK-12 (10 μg/animal) (n=9) and a vehicle (normal saline) -treated disease control group (n =6). TRTK12 was administered via intranasal (IN) route [35]. Anesthetized mice were placed on their backs, and 10 μl solution (containing TRTK12, 1.0 μg/μL or normal saline as vehicle) per mouse was administered through the nose. The subsequent doses were given at 48 hr intervals for 3 weeks. After completion of the treatment, animals were subjected to accelerating rotarod test [35] followed by immunohistochemical and Western blot analysis according to the methods described previously [9]. The Western blot membranes were probed overnight with the appropriate concentration antibodies followed by alkaline phosphatase- labeled secondary antibody and luminescent substrate. The blots were visualized on hyperfilm-ECL (Amersham Biosciences, Buckinghamshire, UK).

### Accelerating rotating rod test

The rotating rod apparatus (Harvard Apparatus, Holliston, MA, USA) was used to measure the ability of mice to improve motor skill performance with training. Starting 24 hr after the completion of last dose mice form the saline and TRTK12 groups were put on the rod (3cm in diameter) for trials 4 times per day for 4 consecutive days. Each trial lasts a maximum of 6–10 min, during which time the rotating rod undergo a linear acceleration from 4 to 40 rpm over the first 5 min of the trial and then remains at maximum speed for the remaining 5 min. Animals rested a minimum of 10 min between trials to avoid fatigue and exhaustion. The mice were scored for their latency to fall (height=20 cm) (in seconds) for each trial. The results were analyzed by a two-way repeated measures ANOVA that factors genotype, day, and trial using GraphPad Prism software, version 4.0 (GraphPad Software, San Diego, CA, USA). A value of $p<0.05$ was accepted as statistically significant.

## Results

### PC S100B vacuole formation correlates with increasing expression of S100B in the SCA1 cerebellum

The appearance of S100B vacuoles in PCs is the earliest morphological change that precedes behavioral abnormalities in SCA1 Tg mice. Similar vacuoles are seen in the surviving PCs

of SCA1 patients [8,9]. In SCA1 Tg mice S100B vacuoles appear between 2 to 3 weeks after birth, which corresponds to a critical period of cerebellar development when BG stop proliferating and begin interacting with PCs [23,24]. To further determine if vacuolar formation is associated with higher expression levels of S100B, we performed expression profiling of S100B mRNA in the cerebellar tissue of 2 and 4 week old SCA1 Tg and age-matched wildtype (WT) mice by using end point PCR and real time PCR techniques. In SCA1 Tg mice, both at 2 and 4 weeks, S100B expression increased significantly as compared to the WT animals (Fig. 1a and b). The data shown in Figure 1b was calculated using the expression of β-actin as a housekeeping gene where relative mRNA levels of S100B were compared to β-actin levels (Fig. 1a). These observations were re-confirmed by real time PCR (Fig. 1c). These data suggest that PC vacuolar formation may be mediated by the increased expression levels of S100B in BG with advancing age.

### S100B localizes to cytoplasm and nucleus in cultured cell lines

S100B is known to have both intracellular and extracellular functions. S100B excreted from astrocytes can target cells externally via binding to the specific receptors or may be internalized and act as an intracellular regulator [36]. To further establish that S100B can be internalized t in cell culture models, we labeled S100B with Alexa-594 fluorescent dye (594-S100B) and treated HeLa cells with varying concentrations of labeled S100B. In agreement with our previous report where we demonstrated that fluorescent labeled S100B localized to the cytoplasm and nucleus of PCs in cerebellar tissue cultures [9], 594-S100B treated HeLa cells showed S100B fluorescence both in the cytoplasm and nucleus (Fig. 2a). In addition, the Western blot analysis of various fractions prepared by treating HeLa cells with 2.0 μM of unlabeled S100B protein showed that S100B localized to both cytosolic and nuclear HeLa cell fractions (Fig. 2b). Furthermore, we created a stable S100B expressing HeLa cell line and observed a similar localization of S100B to the cytoplasm and the nucleus in S100B expressing cells (Fig 3a). These results strengthen our argument that S100B released by BG is internalized by adjacent neurons in the cerebellum.

### S100B increases mutant ataxin-1 solubility

Ataxin-1 is a self-associating nuclear protein that aggregates to form nuclear inclusion bodies [37]. To explore the possibility that S100B may affect mutant ataxin-1 function, we transfected wildtype (WT) HeLa cells and S100B expressing HeLa cell line with GFP-ATXN1[82Q] and monitored changes in mutant ataxin-1 inclusion formation (Fig. 3a and b). Cells expressing GFP-ATXN1[82Q] have been reported to display three phenotypes, soluble nuclear staining, small punctuate foci, and large nuclear inclusions [32,33]. We saw an inverse relation between S100B expression and mutant ataxin-1 inclusion formation. Cells expressing both S100B and GFP-ATXN1[82Q] showed a significant increase in soluble ataxin-1 and a significant reduction in the number of large inclusions as compared to cells expressing GFP-ATXN1[82Q] alone (Fig. 3a and b). We investigated the possibility that S100B and the mutant ataxin-1 protein may be interacting directly by co-immunoprecipitation using lysates of HeLa cells expressing both GFP-ATXN1 and S100B protein. We did not find any direct interaction between these two proteins (data not shown). It could be argued that our results that co-expression of GFP-ATXN1[82Q] and the S100B protein reduces inclusion formation may be due to a competition for protein expression between S100B and GFP-ATXN1. To rule out the possibility of variable protein expression, we produced a GFP-ATXN1[82Q] HEK stable cell line (Fig. 4a) and treated these cells externally with the S100B protein and labeled 594-S100B. 594-S100B treated GFP-ATXN1[82Q] HEK showed a similar S100B localization pattern both to the nucleus and cytoplasm (data not shown) as shown in HeLa cells treated with 594-S100B (Fig. 2a). However, in some GFP-ATXN1[82Q] HEK cells, immunostaining of S100B treated (Fig. 4b) as well as 594-S100B treated cells (Fig. 4c), displayed S100B positive vacuole

formation similar to that seen in SCA1 PCs. Interestingly, the cells with S100B vacuoles lacked nuclear ataxin-1 inclusion bodies (Fig 4b and c). Furthermore, we found that the GFP-ATXN1[82Q] expressing HEK cells showed a significant reduction in number of large inclusions when treated with 250nM S100B (Fig. 4d). S100B treated GFP-ATXN1[82Q] HEK cells showed significantly more small punctuate ataxin-1 foci as compared to the untreated controls. S100B treatment significantly reduced the number of cells with large inclusions by half compare to untreated cells. Furthermore, reduction in the large inclusions was significantly impeded by pre-incubation with S100B inhibitor, TRTK12 (Fig. 4d). TRTK12 peptide has a high binding affinity for S100B with the capabilities to block S100B interaction with it's target proteins [38–40]. The fact that TRTK12 treatment hindered the S100B effect on inclusion size demonstrates that S100B may play a role in mutant ataxin-1 inclusion formation. Take together our data suggest that S100B may reduce mutant ataxin-1 inclusion formation and may increase ataxin-1 solubility through an unknown mechanism.

### SCA1 PCs with S100B vacuoles do not contain ataxin-1 nuclear inclusion bodies

To further explore if the reduction in mutant ataxin-1 inclusions is related with S100B vacuoles *in vivo*, we looked at PCs containing S100B vacuoles and nuclear inclusions in 10 week old SCA1 Tg homozygous mice. This age group was chosen because at this age a significant number of PCs contain ataxin-1 nuclear inclusion bodies. The cerebellar sections were cut in a sagittal plain and for comparison, we counted PCs in the lobes I-III. Interestingly, PCs with S100B vacuoles did not show intranuclear inclusions (Fig. 5a). In 100% of the cells counted, over 50% of PCs had nuclear inclusions and around 20% cells contained S100B vacuoles (Fig. 5b). However, only 3% of PCs had both vacuoles and inclusions (Fig. 5b). These results suggest that SCA1 PCs with S100B vacuoles may contain a more soluble form of ataxin-1. Also, we examined 4 and 6 week old SCA1 Tg heterozygous animals and found that vacuole formation was significantly higher at 6 weeks of age (Fig. 5c), although PC number between 4 and 6 weeks of age was not significantly different in the areas used for PC counting (not shown). Intriguingly, the significant difference in S100B vacuole number in 6 week old animals coincides with age of onset of behavioral deficits in SCA1 Tg mice [6,9]. Furthermore, ataxin-1 nuclear inclusion bodies are rarely seen at this age [6, 9].

### TRTK12 peptide treatment improves SCA1 morphology in cerebellar slice cultures

Previously, we demonstrated that S100B vacuolar formation is associated with alterations in the morphology of dendritic spines of SCA1 PCs [9]. The neurotoxic properties of S100B and its role in neurodegenerative diseases are well documented. Inhibition of S100B proteins may have beneficial effects in SCA1. We investigated the effects of S100B inhibitory peptide TRTK12 on the growth of SCA1 PCs and WT PCs expressing the GFP protein in cerebellar slice cultures. Cultured SCA1 PCs showed morphological changes represented by decreased dendritic arborations as well as dendritic atrophy (Fig. 6a), consistent with those seen *in vivo* [9]. We observed that SCA1 cerebellar cultures grown for different days *in vitro* (DIV) in the presence of 10 μM TRTK12 displayed increased PC dendritic growth compared to untreated cultures (Fig. 6a). In addition, TRTK12 treated SCA1 PC slices showed a significant increase in dendritic length and induction in dendritic branching (Fig. 6c and d). In contrast, TRTK12 treatment had a lesser impact on the growth of GFP WT PC slices (Fig. 6b, c and d).

To further explore the therapeutic properties of the TRTK12 peptide, we administered TRTK12 via IN route to SCA1 Tg mice as previously described [35]. IN administration offers a non-invasive alternative to traditional administration routes (e.g., IV, SC or IM) for the systemic delivery of therapeutics (such as proteins) that are known to possess poor oral bioavailability [41]. Fluorescent labeled TRTK12 peptide when given IN accumulated in the

cerebellum within 2 hrs post-administration in 4 week old SCA1 Tg mice (Fig. 7a), distinctly labeling PCs (Fig. 7b). Neurons in other brain regions also showed differential distribution of TRTK12 (data not shown). Next, 2 week old GFP: SCA1 Tg animals were treated IN with a 10μl solution containing unlabeled TRTK12 or with saline (vehicle) as a control for 3 week period. Interestingly, Western blot analysis of S100B in cerebellar particulate fractions prepared from saline and TRTK12 treated animals showed a significant decrease ($P<0.01$) in S100B levels in the particulate fractions of the TRTK12 treated group (Fig. 8a and b). These data indicate that there may be a lesser S100B translocation to the membranes (to form vacuoles) in the TRTK12 treated group as compared to the saline treated animals. TRTK12 treatment showed no adverse effects on SCA1 animals as evident from the gain in weight presented in the figure 8c. Most intriguing, observation was the improvement of TRTK12 treated animals on the rotarod as compared to the saline treated group (Fig. 8d). An accelerating rotating rod apparatus measures the motor performance ability of the mice during repeated exposure to the task. In summary, our data suggest that glial S100B may influence SCA1 pathology both at the morphologic and molecular level.

## Discussion

Non-cell-autonomous effect of glial cells has been implicated in several neurodegenerative disorders; however, molecular mechanistic pathways involved in the toxicity are currently not identified. In the mouse cerebellum, BG proliferate until the second postnatal week [23,42–44] and this time point overlaps well with the S100B vacuole formation in PCs in a SCA1 Tg mouse [9]. Normal number and function of BG is vital for PC survival [25]. S100B released from glial cells in low concentrations promotes neuronal survival and development, in contrast, higher levels of S100B cause neurotoxicity [13, 14–19]. We also found by expression profiling analysis that the expression of S100B mRNA is increased in the cerebellum in SCA1 mice with increasing postnatal age (Fig: 1). In addition, external addition of S100B or over-expression of S100B in transfected cells carrying mutant ataxin-1 causes reduction in the number of ataxin-1 nuclear inclusions (Fig 3 and 4). Further, using cerebellar slice cultures and in vivo treatment of SCA1 Tg mice with S100B inhibitory peptide TRTK12 we showed that inhibition of S100B function caused reversal of S100B mediated effects and improved behavior deficits. Furthermore, our preliminary studies on genome-wide cerebellar gene expression profiling have shown that the expression of BG and PC specific genes involved in cell-adhesion, signaling and guidance are significantly dysregulated in 2wk old SCA1 mice (unpublished observations). Therefore, we speculate that the sustained expression of mutant ataxin-1 as a transcriptional repressor may generate a stress signal, which causes BG to react and release high levels of S100B protein. S100B has been used as a marker for brain injury [45]. Elevated levels of S100B in response to neuronal dysfunction have been reported in many neurodegenerative disorders including Down syndrome and Alzheimer disease [14, 18]. Further, Gerlach and co-workers [46] using astrocyte cultures showed that astrocytes actively secrete S100B during metabolic stress. In sum, the above observations indicate that BG may be the up-stream site of ataxin-1 mediated pathology in SCA1.

Ataxin-1 is a self-associating protein, where removal of the self-associating domain prevents mutant ataxin-1 inclusion formation [37]. SCA1 Tg mice expressing mutant ataxin-1 lacking the self-association domain develop progressive ataxia similar to B05 SCA1 Tg mice that contain the intact self-association domain [37]. The soluble form of the mutant ataxin-1 protein has been suggested as the neurotoxic form of the misfolded protein [37, 47]. Therefore, processes that increase mutant ataxin-1 solubility could be considered as modulators of ataxin-1 neurotoxicity. Watase and co-workers [47] targeted 154 CAG repeats into the endogenous mouse locus. SCA1(154Q/2Q) mice developed a progressive neurological disorder accompanied by PC loss and age-related hippocampal synaptic

dysfunction. Mutant ataxin-1 solubility varied with brain region, being most soluble in the neurons most vulnerable to degeneration especially PCs [47]. Furthermore, we and others have shown earlier in B05 SCA1 Tg mice, that several essential PC proteins are down-regulated prior to the appearance of intranuclear inclusions [48–50]. Interestingly, ataxin-1 has been shown to interact with a whole host of transcription factors, furthermore ataxin-1 has been shown to occupy the Dopamine 2 receptor (D2R) promoter to co-regulate D2R gene expression [51]. It is enticing to think that BG may play some part in regulating mutant ataxin-1 solubility enhancing PC degeneration. This argument is supported by the fact that PCs containing S100B vacuoles lack ataxin-1 nuclear inclusions (Fig 5) and these cells are usually at higher degenerative state as indicated by dendritic and spine abnormalities [9].

S100B is constitutively secreted by astrocytes and its secretion can be regulated by a number of factors [36]. Accumulating evidence suggests that intracellular regulatory activities of S100B differ substantially from its extracellular effects [52–55]. We believe that glial S100B internalized in PCs may be affecting physiologic processes vital for PC survival as indicated by our previous study where we found that S100B in PC vacuoles is co-localized with IMPase 1, an important enzyme regulating inositol 1, 4, 5 trisphosphate signaling in PCs [9]. S100B protein also regulates nuclear Dbf2-related 2 (NDR2) protein kinase by stimulating its autophosphorylation [56]. NDR2 belongs to the subfamily of serine/threonine kinases that control cell division and morphogenesis in various cell types, including neurons [57,58]. NDR2 is highly expressed in cerebellar PCs and show a predominant cytoplasmic localization [56]. Stork et al [58] studied the function of NDR2 on neurite growth and reported that NDR2 negatively regulates substrate adhesion in differentiated PC12 cells, possibly by reducing the stability of actin-dependent contact sites. We speculate that sustained presence S100B vacuoles in differentiating PCs in SCA1 may act as a constant source of S100B to activate PC NDR2 kinase, which in an activated state destabilizes BG-PC contact sites and neurite growth resulting in PC degeneration. A stronger argument suggesting the S100B involvement in SCA1 neurodegeneration comes from the beneficial effects of TRTK12 both on SCA1 slice cultured PCs and IN treated SCA1 Tg mice (Fig 6 and 7). The fact that S100B inhibition improves SCA1 phenotype, suggests that BG S100B may play a key role in the SCA1 neurodegenerative pathway. Further, understanding the molecular mechanisms underlying the glial-neuronal crosstalk will help develop novel therapeutics against the non-autonomous polyglutamine pathology in multiple polyglutamine diseases.

## Acknowledgments

This work was supported in part by a grant from the National Ataxia Foundation.

## References

1. Koeppen AH. The pathogenesis of spinocerebellar ataxia. Cerebellum. 2005; 4:62–73. [PubMed: 15895563]
2. Matilla-Duen as A, Goold R, Giunti P. Clinical, genetic, molecular, and pathophysiological insights into Spinocerebellar ataxia type 1. Cerebellum. 2007; 7:1–9.
3. Orr HT, Zoghbi HY. Trinucleotide repeat disorders. Annu Rev Neurosci. 2007; 30:575–621. [PubMed: 17417937]
4. Banfi S, Servadio A, Chung MY, Kwiatkowski TJ Jr, McCall AE, Duvick LA, et al. Identification and characterization of the gene causing type 1 spinocerebellar ataxia. Nat Genet. 1994; 7:513–520. [PubMed: 7951322]
5. Duvick L, Barnes J, Ebner B, Agrawal S, Andresen M, Lim J, Giesler GJ, Zoghbi HY, Orr HT. SCA1-like disease in mice expressing wild-type ataxin-1 with a serine to aspartic acid replacement at residue 776. Neuron. 2010; 67:929–35. [PubMed: 20869591]

6. Burright EN, Clark HB, Servadio A, Matilla T, Feddersen RM, Yunis WS, et al. SCA-1 transgenic mice: a model for neurodegeneration caused by an expanded CAG trinucleotide repeat. Cell. 1995; 82:937–948. [PubMed: 7553854]
7. Skinner PJ, Vierra-Green CA, Clark HB, Zoghbi HY, Orr HT. Altered trafficking of membrane proteins in Purkinje cells of SCA1 transgenic mice. Am J Pathol. 2001; 159:905–913. [PubMed: 11549583]
8. Vig PJS, Lopez ME, Wei J, D'Souza DR, Subramony SH, Henegar J, et al. Glial S100B positive vacuoles in Purkinje cells: earliest morphological abnormality in SCA1 transgenic mice. J Neurol Sci [Turk]. 2006; 23:166–174.
9. Vig PJ, Shao Q, Subramony SH, Lopez ME, Safaya E. Bergmann glial S100B activates myo-inositol monophosphatase 1 and Co-localizes to purkinje cell vacuoles in SCA1 transgenic mice. Cerebellum. 2009; 8:231–244. [PubMed: 19593677]
10. Donato R. Perspectives in S-100 protein biology. Cell Calcium. 1991; 12:713–726. [PubMed: 1769063]
11. Zimmer DB, Chaplin J, Baldwin A, Rast M. S100-mediated signal transduction in the nervous system and neurological diseases. Cell Mol Biol. 2005; 51:201–214. [PubMed: 16171556]
12. Reeves RH, Yao J, Crowley MR, Buck S, Zhang X, Yarowsky P, et al. Astrocytosis and axonal proliferation in the hippocampus of S100b transgenic mice. Proc Natl Acad Sci U S A. 1994; 91:5359–5363. [PubMed: 8202493]
13. Huttunen HJ, Kuja-Panula J, Sorci G, Agneletti AL, Donato R, Rauvala H, et al. Coregulation of neurite outgrowth and cell survival by amphoterin and S100 proteins through receptor for advanced glycation end products (RAGE) activation. J Biol Chem. 2000; 275:40096–40105. [PubMed: 11007787]
14. Rothermundt M, Peters M, Prehn JH, Arolt V. S100B in brain damage and neurodegeneration. Microsc Res Tech. 2003; 60:614–632. [PubMed: 12645009]
15. Winningham-Major F, Staecker JL, Barges SW, Coats S, VanElkik J. Neurite extension and neuronal survival activities of recombinant S100β proteins that differ in the content and position of cysteine residues. J Cell Biol. 1989; 109:3064–3071.
16. Barger SW, VanEldik LJ, Mattson MP. S100β protects hippocampal neurons from damage induced by glucose deprivation. Brain Res. 1995; 677:167–170. [PubMed: 7606463]
17. Whitaker-Azmitia PM, Vingate M, Borella A, Gerlai R, Roder J, Azmitia EC. Transgenic mice overexpressing the neurotrophic factor S-100β show neuronal cytoskeletal and behavioral signs of altered aging processes: implications for Alzheimer's disease and Down's syndrome. Brain Res. 1997; 776:51–60. [PubMed: 9439795]
18. Griffin WS, Stanley LC, Ling C, White L, MacLeod V, Perrot LJ, et al. Brain interleukin 1 and S-100 immunoreactivity are elevated in Down syndrome and Alzheimer disease. Proc Natl Acad Sci U S A. 1989; 86:7611–7615. [PubMed: 2529544]
19. Kato K, Suzuki F, Kurobe N, Okajima K, Ogasawara N, Nagaya M, et al. Enhancement of S-100β protein in blood of patients with Down's syndrome. J Mol Neurosci. 1990; 2:109–113. [PubMed: 2150320]
20. Donato R. Functional roles of S100 proteins, calcium binding proteins of the EF-hand type. Biochim Biophys Acta. 1999; 1450:191–231. [PubMed: 10395934]
21. McClintock KA, Shaw GS. A logical sequence search for S100B target proteins. Protein Sci. 2000; 10:2043–2046. [PubMed: 11106180]
22. Wilder PT, Lin J, Bair CL, Charpentier TH, Yang D, Liriano M, et al. Recognition of the tumor suppressor protein p53 and other protein targets by the calcium-binding protein S100B. Biochim Biophys Acta. 2006; 1763:1284–1297. [PubMed: 17010455]
23. Yamada K, Watanabe M. Cytodifferentiation of Bergmann glia and its relationship with Purkinje cell. Anat Sci Int. 2002; 2:94–108. [PubMed: 12418089]
24. Hoogland TM, Kuhn B. Recent developments in the understanding of astrocyte function in the cerebellum in vivo. Cerebellum. 2010; 9:264–271. [PubMed: 19904577]
25. Delaney CL, Brenner M, Messing A. Conditional ablation of cerebellar astrocytes in postnatal transgenic mice. J Neurosci. 1996; 16:6908–6918. [PubMed: 8824329]

26. Shiwaku H, Yoshimura N, Tamura T, Sone M, Ogishima S, Watase K, Tagawa K, Okazawa H. Suppression of the novel ER protein Maxer by mutant ataxin-1 in Bergman glia contributes to non-cell-autonomous toxicity. EMBO J. 2010; 29:2446–2460. [PubMed: 20531390]
27. Custer SK, Garden GA, Gill N, Rueb U, Libby RT, Schultz C, Guyenet SJ, Deller T, Westrum LE, Sopher BL, La Spada AR. Bergmann glia expression of polyglutamine-expanded ataxin-7 produces neurodegeneration by impairing glutamate transport. Nat Neurosci. 2006; 9:1302–1311. [PubMed: 16936724]
28. Cummings CJ, Mancini MA, Antalffy B, DeFranco DB, Orr HT, Zoghbi HY. Chaperone suppression of aggregation and altered subcellular proteasome localization imply protein misfolding in SCA1. Nat Genet. 1998; 19:148–154. [PubMed: 9620770]
29. Emamian ES, Kaytor MD, Duvick LA, Zu T, Tousey SK, Zoghbi HY, Clark HB, Orr HT. Serine 776 of ataxin-1 is critical for polyglutamine-induced disease in SCA1 transgenic mice. Neuron. 2003; 38:375–387. [PubMed: 12741986]
30. Chen HK, Fernandez-Funez P, Acevedo SF, et al. Interaction of Akt-phosphorylated ataxin-1 with 14-3-3 mediates neurodegeneration in spinocerebellar ataxia type 1. Cell. 2003; 113:457–468. [PubMed: 12757707]
31. Liu Y, Buck DC, Neve KA. Novel interaction of the dopamine D2 receptor and the Ca2+ binding protein S100B: role in D2 receptor function. Mol Pharmacol. 2008; 74:371–378. [PubMed: 18445708]
32. Parfitt DA, Michael GJ, Vermeulen EG, Prodromou NV, Webb TR, Gallo JM, Cheetham ME, Nicoll WS, Blatch GL, Chapple JP. The ataxia protein sacsin is a functional cochaperone that protects against polyglutamine-expanded ataxin-1. Hum Mol Genet. 2009; 18:1556–1565. [PubMed: 19208651]
33. Hearst SM, Lopez ME, Shao Q, Liu Y, Vig PJ. Dopamine D2 receptor signaling modulates mutant ataxin-1 S776 phosphorylation and aggregation. J Neurochem. 2010; 114:706–716. [PubMed: 20477910]
34. Livak KJ, Schmittgen TD. Analysis of relative gene expression data using real-time quantitative PCR and the 2(-Delta Delta C(T)) Method. Methods. 2001; 25:402–408. [PubMed: 11846609]
35. Vig PJS, Subramony SH, D'Souza DR, Wei J, Lopez ME. Intranasal administration of IGF-I improves behavior and Purkinje cell pathology in SCA1 mice, Brain Res. Bull. 2006; 69:574–579.
36. Donato R, Sorci G, Riuzzi F, Arcuri C, Bianchi R, Brozzi F, Tubaro C, Giambanco I. S100B's double life: intracellular regulator and extracellular signal. Biochim Biophys Acta. 2009; 1793:1008–1022. [PubMed: 19110011]
37. Klement IA, Skinner PJ, Kaytor MD, Yi H, Hersch SM, Clark HB, Zoghbi HY, Orr HT. Ataxin-1 nuclear localization and aggregation: role in polyglutamine-induced disease in SCA1 transgenic mice. Cell. 1998; 95:41–53. [PubMed: 9778246]
38. Ivanenkov VV, Jamieson GA Jr, Gruenstein E, Dimlich RV. Characterization of S-100b binding epitopes. Identification of a novel target, the actin capping protein, CapZ. J Biol Chem. 1995; 270:14651–14658. [PubMed: 7540176]
39. Bianchi R, Garbuglia M, Verzini M, Giambanco I, Ivanenkov VV, Dimlich RV, Jamieson GA Jr, Donato R. S-100 (alpha and beta) binding peptide (TRTK-12) blocks S-100/GFAP interaction: identification of a putative S-100 target epitope within the head domain of GFAP. Biochim Biophys Acta. 1996; 1313:258–267. [PubMed: 8898863]
40. Charpentier TH, Thompson LE, Liriano MA, et al. The effects of CapZ peptide (TRTK-12) binding to S100B-$Ca^{2+}$ as examined by NMR and X-ray crystallography. J Mol Biol. 2010; 396:1227–1243. [PubMed: 20053360]
41. Thorne RG, Pronk GJ, Padmanabhan V, Frey WH 2nd. Delivery of insulin-like growth factor-I to the rat brain and spinal cord along olfactory and trigeminal pathways following intranasal administration. Neuroscience. 2004; 127:481–496. [PubMed: 15262337]
42. Basco E, Hajos F, Fulop Z. Proliferation of Bergmann-glia in the developing rat cerebellum. Anat Embryol (Berl). 1977; 151:219–222. [PubMed: 920969]
43. Shiga T, Ichikawa M, Hirata Y. Spatial and temporal pattern of postnatal proliferation of Bergmann glial cells in rat cerebellum: anautoradiographic study. Anat Embryol (Berl). 1983; 167:203–211. [PubMed: 6614505]

44. Gaiano N, Fishell G. The role of notch in promoting glial and neural stem cell fates. Annu Rev Neurosci. 2002; 25:471–490. [PubMed: 12052917]
45. Ellis EF, Willoughby KA, Sparks SA, Chen T. S100B protein is released from ratneonatal neurons, astrocytes, and microglia by in vitro trauma and anti-S100 increases trauma-induced delayed neuronal injury and negates the protective effect of exogenous S100B on neurons. J Neurochem. 2007; 101:1463–1470. [PubMed: 17403138]
46. Gerlach R, Demel G, König HG, Gross U, Prehn JH, Raabe A, Seifert V, Kögel D. Active secretion of S100B from astrocytes during metabolic stress. Neuroscience. 2006; 141:1697–1701. [PubMed: 16782283]
47. Watase K, Weeber EJ, Xu B, Antalffy B, Yuva-Paylor L, Hashimoto K, Kano M, Atkinson R, Sun Y, Armstrong DL, Sweatt JD, Orr HT, Paylor R, Zoghbi HY. A long CAG repeat in the mouse Sca1 locus replicates SCA1 features and reveals the impact of protein solubility on selective neurodegeneration. Neuron. 2002; 34:905–919. [PubMed: 12086639]
48. Lin X, Antalffy B, Kang D, Orr HT, Zogbi HY. Polyglutamine expansion down-regulates specific neuronal genes before pathologic changes in SCA1. Nature Neurosci. 2000; 3:157–163. [PubMed: 10649571]
49. Vig PJS, Subramony SH, Qin Z, McDaniel DO, Fratkin J. Relationship between ataxin-1 nuclear inclusions and Purkinje cell specific proteins in SCA-1 transgenic mice. J Neurol Sci. 2000; 174:100–110. [PubMed: 10727695]
50. Goold R, Hubank M, Hunt A, Holton J, Menon RP, Revesz T, Pandolfo M, Matilla-Duenas A. Down-regulation of the dopamine receptor D2 in mice lacking ataxin-1. Hum Mol Genet. 2007; 17:2122–2134. [PubMed: 17599952]
51. Tubaro C, Arcuri C, Giambanco I, Donato R. S100B protein in myoblasts modulates myogenic differentiation via NF-κB-dependent inhibition of MyoD expression. Journal of Cellular Physiology. 2010; 223:270–282. [PubMed: 20069545]
52. Saito T, Ikeda T, Nakamura K, Chung U-I, Kawaguchi H. S100A1 and S100B, transcriptional targets of SOX trio, inhibit terminal differentiation of chondrocytes. EMBO Reports. 2007; 8:504–509. [PubMed: 17396138]
53. Brozzi F, Arcuri C, Giambanco I, Donato R. S100B Protein Regulates Astrocyte Shape and Migration via Interaction with Src Kinase: Implications for astrocyte development, activation and tumor growth. J Biol Chem. 2009; 284:8797–8811. [PubMed: 19147496]
54. Sorci G, Bianchi R, Riuzzi F, Tubaro C, Arcuri C, Giambanco I, Donato R. S100B Protein, A Damage-Associated Molecular Pattern Protein in the Brain and Heart, and Beyond. Cardiovasc Psychiatry Neurol. 2010 pii: 656481.
55. Stegert MR, Tamaskovic R, Bichsel SJ, Hergovich A, Hemmings BA. Regulation of NDR2 protein kinase by multi-site phosphorylation and the S100B calcium-binding protein. J Biol Chem. 2004; 279:23806–23812. [PubMed: 15037617]
56. Kandel ER. The molecular biology of memory storage: a dialogue between genes and synapses. Science. 2001; 294:1030–1038. [PubMed: 11691980]
57. Stork O, Zhdanov A, Kudersky A, Yoshikawa T, Obata K, Pape HC. Neuronal functions of the novel serine/threonine kinase Ndr2. J Biol Chem. 2004; 279:45773–45781. [PubMed: 15308672]

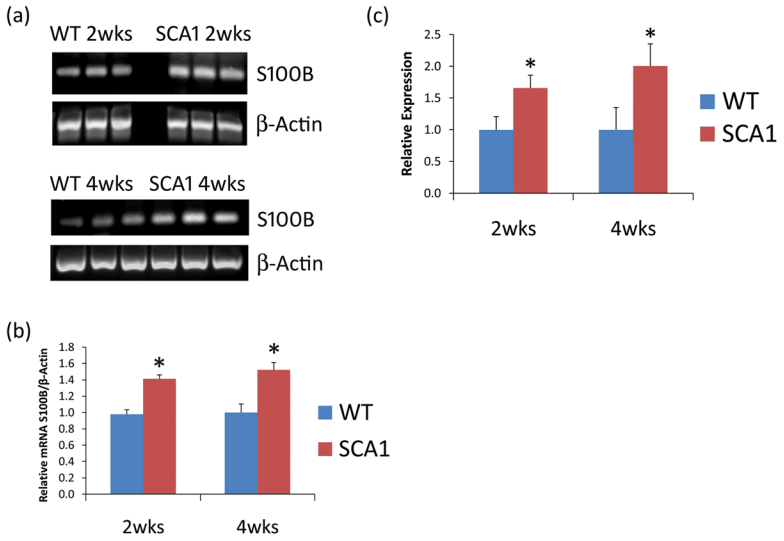


**Figure 1.**

(a) Shown is an image of the end point PCR results after 30 cycles of amplification for both S100B and β-Actin cerebellar cDNA from 2 and 4 wk old WT and SCA1 Tg mice. Band intensities were taken using Image J software and used to estimate the mRNA levels of S100B compared to β-Actin for each group. (b) Graph displays the MEAN±SE of the Relative mRNA levels of S100B compared to β-Actin. (c) Graph displays the MEAN±SE of the relative gene expression of S100B among the different groups using real time PCR technique, where β-Actin was used as the housekeeping gene. Statistical significance was calculated using the Student's t-test. S100B mRNA levels are significantly up-regulated in the cerebellum of SCA1 mice compared to WT mice of the same background, *P<0.01.

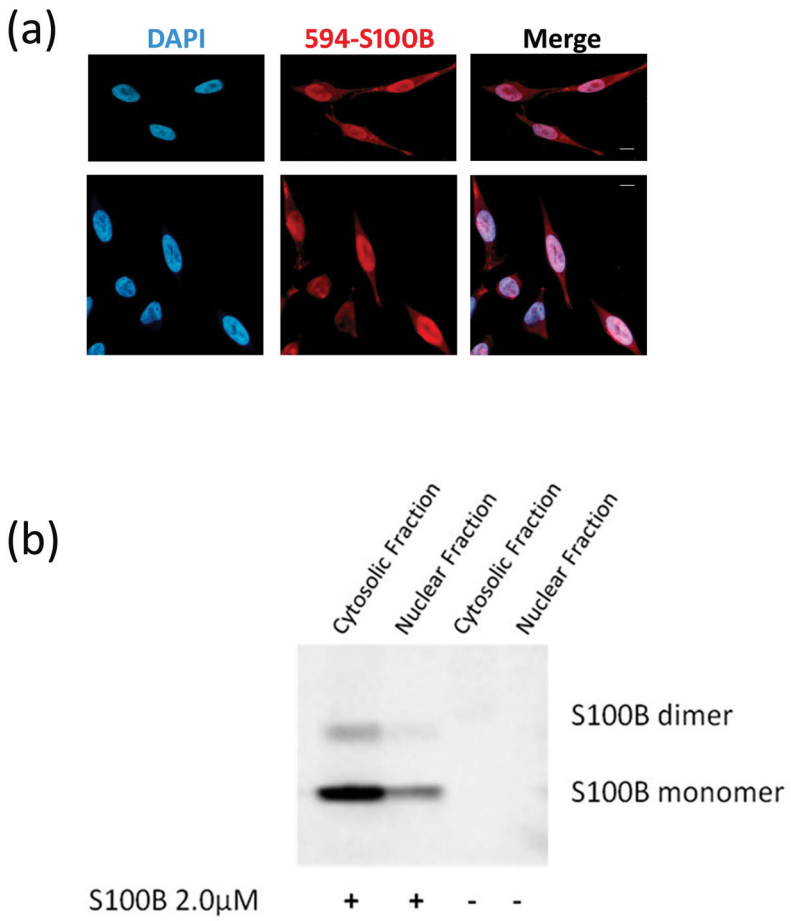


**Figure 2.**

(a) HeLa cells were transferred to 2 well slides and treated with 2.0 μM 594-S100B for 6hrs followed by fixation and DAPI staining. Fluorescent microscopy displays DAPI nuclear staining in blue and 594-S100B in red. Scale bars: 10 μm. (b) HeLa cells were transferred to 6 well plates and treated with 2.0μM unlabeled S100B protein for 6hrs. Cells were washed with PBS and lysed in the plates using Nuclear/Cytosol Fractionation Kit (BioVision, Mountain View, CA, USA) according to the manufacture's protocol. Isolated nuclear and cytosolic fractions were subject to Western blotting followed by detection using S100B antibody. S100B localized both to the nucleus and cytoplasm of HeLa cells.

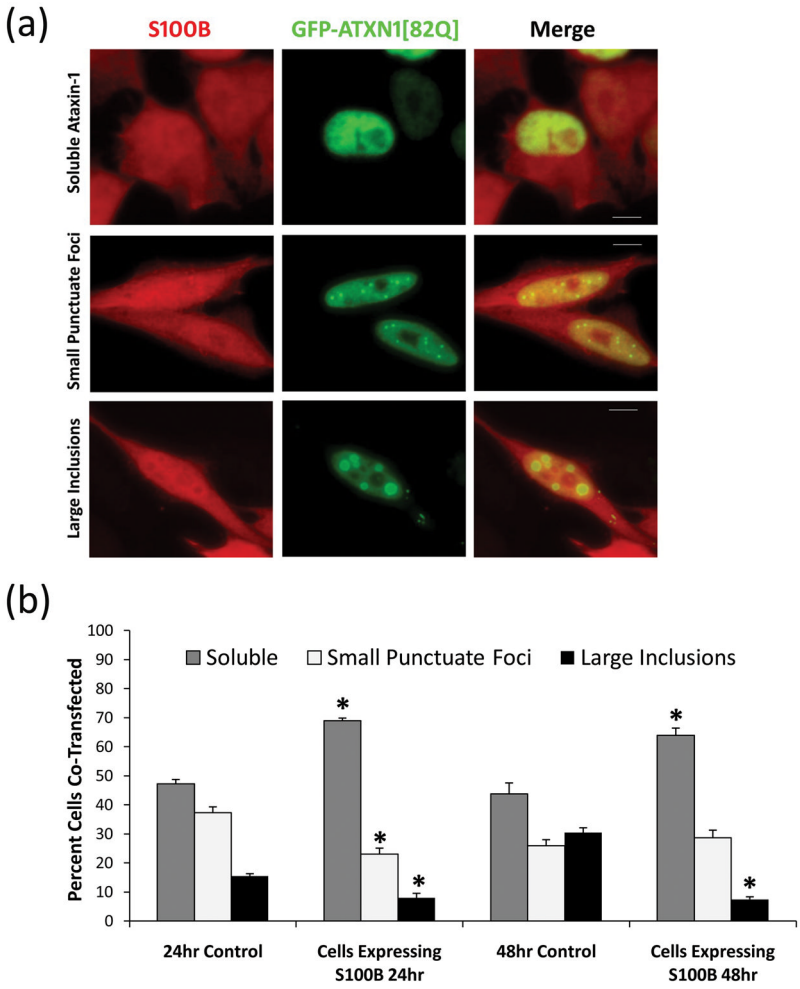


**Figure 3.**

S100B expressing HeLa cells or non-expressing HeLa cells (control, not shown) were transfected with GFP-ATXN1[82Q]. (a) Image shows GFP-ATXN1[82Q] in green and S100B in red, where cells display soluble nuclear GFP-ATXN1[82Q], small punctuate GFP-ATXN1[82Q] foci and large GFP-ATXN1[82Q] inclusion bodies. (b) Cells were scored as soluble ataxin-1, small punctuate ataxin-1 foci, or large ataxin-1 inclusions as described previously [33], 24hrs and 48hrs post-transfection. Data is represented as Mean ± SE. Statistical significance was calculated using Student's t-test. *Ctrl vs Cells Expressing S100B, $P<0.01$. Scale bars: 10μm.

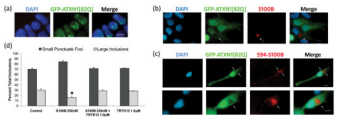

**Figure 4.**

(a) GFP-ATXN1[82Q] HEK stable cells showing shows DAPI nuclear stain in blue and GFP-ATXN1[82Q] in green. GFP-ATXN1[82Q] HEK stable cells were transferred to 2 well slides and treated with (b) 500nM S100B protein for 24hrs followed by fixation and immunostaining and (c) treated with 500nM 594-S100B for 24hrs followed by fixation. Fluorescent staining shows DAPI nuclear stain in blue, GFP-ATXN1[82Q] in green, and S100B or 594-S100B in red. In less than 10% of cells, S100B treatments resulted in vacuolar formations, indicated by arrows, similar to those seen in SCA1 PCs [6,9]. Scale bars: 10μm. (d) HEK GFP-ATXN1[82Q] stable line was treated for 24hrs with 2% FBS as control, with 250nM S100B, 250nM S100B + 1μM TRTK12, or with 1μM TRTK12 alone. Cells expressing ataxin-1 inclusions were scored as small punctuate foci or large inclusions as described previously [33]. Data is presented as MEAN ±SE. Statistical significance was calculated using the Student's t-test. *S100B vs Ctrl or S100B vs S100B + TRTK12: $P < 0.005$. Ctrl vs S100B + TRTK12 or Ctrl vs TRTK12: $P > 0.5$.

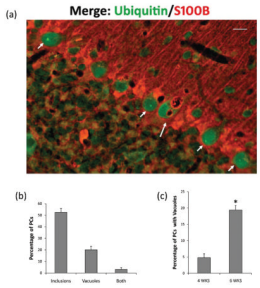


**Figure 5.**

(a) Double immunofluorescence showing ubiquitinated ataxin-1 inclusions (green) in PCs and S100B (red) in BG in 10 wks old SCA1 Tg homozygous mouse. PC with S100B vacuole (large arrow) does not contain nuclear inclusions (small arrows). Scale bar: 25μm. (b) Data shows the percentage of PCs with nuclear inclusion, S100B vacuoles or both from 10 week old SCA1 homozygous mice (n=4). Data is represented as MEAN±SE. (c) Data shows the percentage of PCs with S100B vacuoles in 4 (n=5) and 6 week (n =5) old SCA1 Tg heterozygous mice. PCs in lobes I-III were counted using cerebellar sections from different animals. Data is represented as MEAN±SE. Statistical significance was calculated using the Student's t-test, *4 wks vs 6wks, $P<0.01$.

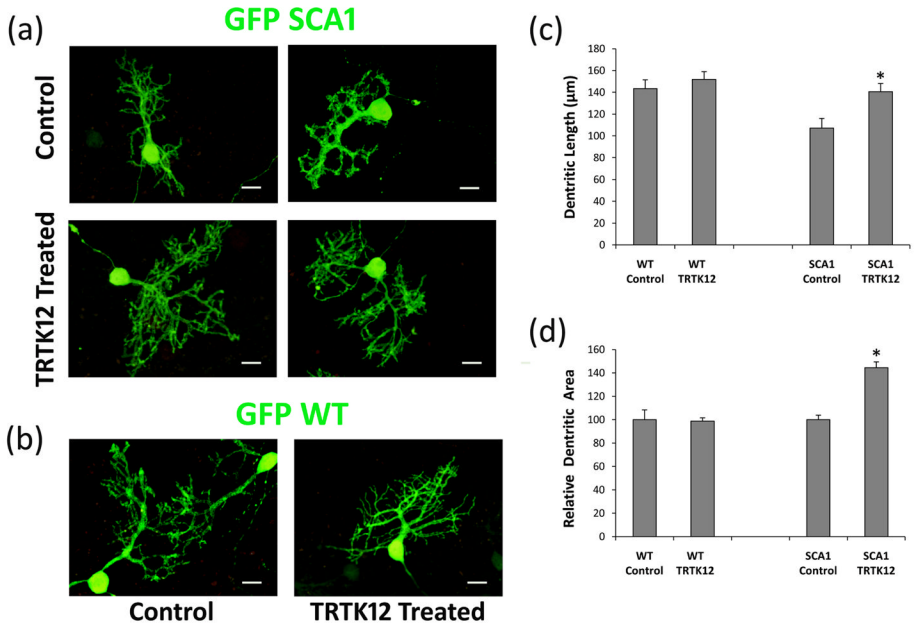


**Figure 6.**

GFP immunofluorescence of organotypic cerebellar slice cultures prepared from 7 day old GFP: SCA1 Tg and GFP: WT mice. (a) 250 µm thick slices were grown on Millicell membrane inserts using 6 well culture plates. One day in vitro (DIV) old slices were grown in the culture media with or without 10 µM TRTK12 for 21 DIV followed by fixation and immunocytochemistry. The digitized images show abnormally developed dendritic processes in SCA1 slices without TRTK12 as compared with SCA1 slices treated with TRTK12. (b) TRTK12 showed no effect in WT PCs grown in the media containing TRTK12 compare to WT controls. (c) The digitized images were used to compare PC dentritic lengths after TRTK12 treatment. Dentrites were measured (n=40) using Image J software. Data is displayed as MEAN±SE. *P<0.01. (d) The digitized images were used to compare total PC dentritic branch area after TRTK12 treatment. Dentritic areas were measured (n=16) using Image J software, where the total dentritic branch area was taken by converting the image to black pixels and analyzing the total pixel area for each PC. The data was then normalized to the controls, where control values are equal to 100. Data is displayed as MEAN±SE. Statistical significance was calculated using the Student t-test. SCA1 Control vs SCA1 TRTK12, *P<0.01.

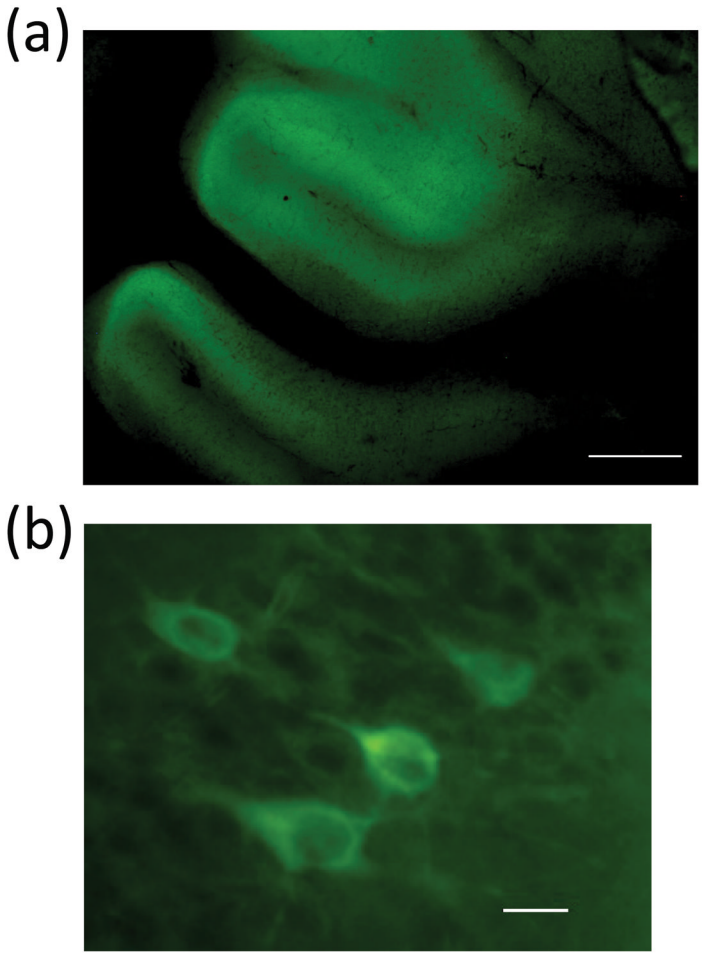


**Figure 7.**

5FAM labeled TRTK12 peptide fluorescence in the cerebellar section of TRTK12 treated (IN) 4 week old SCA1 Tg homozygous mouse. These animals were administered 50 μg/10 μl of 5FAM-TRTK12. Animals were sacrificed after 2 hr post-treatment. Brains were perfusion fixed and sectioned. PCs in the multi-layered PC layer are visible (green) at (a) low magnification, scale bar: 300 μm and (b) high magnification, scale bar: 10 μm.

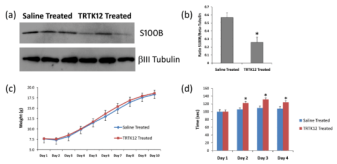


**Figure 8.**

(a) Western blots showing S100B and beta III tubulin in the cerebellar particulate fractions prepared from SCA1 Tg saline (n=3) and TRTK12 treated (n=3) animals. (b) The S100B-Tubulin band intensity ratios were calculated using Image J software. A significant decrease (*P<0.01) in S100B levels (in the particulate fractions) were observed after TRTK12 treatment. Student's t-test for independent samples was used for calculating statistically significant differences (GraphPad Prism Software). The data are presented as the Mean± SE. (c) Graph shows the changes in the body weight during IN normal saline and TRTK12 treatments to SCA1 Tg animals. No significant differences in the body weight were observed. (d) Rotarod test of SCA1 Tg mice treated IN with saline and TRTK12. A minimum of 6 animals/group were used. Mice were subjected to 4 trials/day for 4 consecutive days. The data was normalized to 100 for the performance on Day 1. The results are presented as the Mean±SE. Two way ANOVA with Bonferroni posttest was used for calculating statistically significant differences (GraphPad Prism Software). *Saline Treated vs TRTK12 Treated, P<0.01.